指す。

F. 研究発表

1. 論文発表

1. Zhao, Y., Takahashi, M., **Gu, J.**, Miyoshi, E., Matsumoto, A., Kitazume, S. and Taniguchi, N. Functional roles of N-glycans in cell signaling and cell adhesion in cancer (2008) *Cancer Sci* 99, 1304-10.
2. **Gu, J.** and Taniguchi, N. Potential of N-glycan in cell adhesion and migration: As either a positive or negative regulator (2008) *Cell Adhesion & Migration* 2, 1-3.
3. **Gu, J.**, Sato, Y., Kariya, Y., Isaji, T., Taniguchi, N. and Fukuda, T. A mutual regulation between cell-cell adhesion and N-glycosylation: implication of the bisecting GlcNAc for biological functions (2008) *J. Proteome Res.* 8, 431-435.
4. Osumi, D., Takahashi, M., Miyoshi, E., Yokoe, S., Lee, SH., Noda, K., Nakamori, S., **Gu, J.**, Ikeda, Y., Kuroki, Y., Sengoku, K., Ishikawa, M. and Taniguchi, N. Core fucosylation of E-cadherin enhances cell-cell adhesion in human colon carcinoma WiDr cells (2009) *Cancer Sci* 99, 1304-1310.
5. Wang, X., Fukuda, T., Li, W., Gao, C., Kondo, A., Matsumoto, A., Miyoshi, E., Taniguchi, N. and **Gu, J.** Requirement of Fut8 for the expression of vascular endothelial growth factor receptor-2: a new mechanism for the emphysema-like changes observed in Fut8-deficient mice (2009) *J. Biochem.* In press.
6. Isaji, T., Sato, Y., Fukuda,T. and **Gu, J.** N-glycosylation of the I-like domain of beta1 integrin is essential for beta1 integrin expression and biological function: Identification of the minimal N-glycosylation requirement for alpha 5beta 1. (2009) *J. Biol. Chem.* In press.
7. Sato, Y., Isaji, T., Tajiri, M., Yoshida-Yamamoto, S., Yoshinaka, T., Somehara, T., Fukuda, T., Wada, Y. and **Gu, J.** An N-glycosylation site on the beta-propeller domain of the integrin alpha5 subunit plays key roles in both its function and site-specific modification by beta 1,4-N-acetylglucosaminyltransferase III (2009) *J. Biol. Chem.* In press.

2. 学会発表

1. 糖鎖によるインテグリンの機能調節. 伊左治知弥、佐藤裕也、福田友彦、顧建国; 日本生化学会東北支部第 73 回例会・シンポジウム; 東北大学医学部艮陵会館; 2007 年 5 月 12 日
2. N-結合型糖鎖によるインテグリンとその複合体形成の機能制御. 顧 建国; 第 30 回年日本分子生物学会・第 80 回生化学会合同会議; 横浜; 2007 年 12 月 11-15 日
3. N 分岐型糖鎖修飾の意義について. 顧 建国; 第一回東北糖鎖研究会; 東北薬科大学; 2007 年 12 月 22-23 日

4. Fut8 の機能解析:疾患とコアフコース.顧 建国;高知システム糖鎖生物学教育研究センター第一回公開シンポジウム『糖鎖と医学の関わり』、高知大学医学部;2008 年 3 月 21 日
5. Fut8 欠損マウスにおける統合失調症様行動 福田友彦、顧建国「第 28 回日本糖質学年会」茨城県つくば 2008 年 8 月 18-20 日
6. 糖転移酵素 Fut8 と肺気腫 顧建国「第 4 回産業医科大学大学院シンポジウム」 産業医科大学ラマチーニホール 2008 年 10 月 16 日
7. インテグリンの N-結合型糖鎖による細胞接着機能の制御 顧建国「日本第6回糖鎖科学コンソーシアムシンポジウム」 東京コンファレンスセンター品川 2008 年 12 月 3,4 日
8. A Schizophrenia-like behavior in the Fut8-deficient mouse. 顧建国 「Frontiers in Glycomics workshop」 The Shanghai Centre for Systems Biomedicine, Shanghai Jiao Tong University, China 2009 年 1 月 4,5 日
9. Roles of N-glycosylation in integrin biological functions. 顧建国 東北糖鎖研究会サテライトシンポジウム コラッセふくしま、福島 2009 年 3 月 21 日

2. 実用新案登録

該当なし

3.その他

該当なし

G.. 知的財産権の出願・登録状況(予定を含む。)

1. 特許取得

該当なし

厚生労働科学研究費補助金（創薬基盤推進研究事業）
分担研究報告書

エラスターゼ誘導肺気腫モデルにおけるFUT8+/-♂マウスの検討

分担研究者　別役　智子　北海道大学大学院医学研究科　准教授

研究要旨 FUT8mRNA の発現が低下している FUT8 ヘテロマウスを用いて、エラスターゼ誘導肺気腫モデルにおける野生型との差を検討した。エラスターゼ気管内投与により FUT8 ヘテロマウスでは野生型と比較して早期に気腫化がおこり、エラスターゼ投与後 14 日および 21 日目の肺においてより強い肺気腫を認めた。エラスターゼ投与 24 時間後の気管支肺胞洗浄液中の MMP2 活性は FUT8 ヘテロマウスでより強かった。FUT8 ヘテロマウスでより早期に気腫が起きる機序としてエラスターゼ投与に対する MMP 活性がヘテロマウスにおいて亢進している可能性が考えられた。

A. 研究目的

エラスターゼ誘導肺気腫モデルとは、ブタ膵エラスターゼを気道に注入することで、直接的にエラスチン分解と炎症を惹起し、呼吸生理学的・病理組織学的にヒトの肺気腫病変に類似したモデルを得られることが確立している。昨年度、我々は野生型と FUT8 ヘテロマウスを用いた本モデルの検討においてエラスターゼ投与後 21 日において、FUT8 ヘテロマウスは、野生型マウスに比較し、気腫化の程度が強いことを報告した。今年度は、同モデルを用いて、より早期の段階でも、FUT8 ヘテロマウスと野生型マウスの気腫化の程度に差があるかどうか、またその機序にマトリックスメタロプロテアーゼ（matrix metalloproteinase; MMP）の多寡が関与しているか否か、修復機転に関してエラスチン、コラーゲン産生能に差があるか否かを検討した。

B. 研究方法

週齢 10～11 週のオス FUT8+/-マウスと、対照として週齢と性別を合わせた野生型 C57/B6 マウスを用いる。MicroSprayer® (Penn-Century Inc.)を用いて、ブタ膵エラスターゼ（pancreatic porcine elastase, EC134, Elastin Products)を 3U、または生理的食塩水を気管内噴霧投与する。投与前、投与 3 時間、24 時間、7 日、14 日、21 日後、42 日後、63 日後の各々のタイムポイントで屠殺する。各群 5-6 匹ずつとし、気管支肺胞洗浄(bronchoalveolar lavage: BAL)と凍結肺標本作成を行う。BAL 液について gelatin zymography をおこない、BAL 液中の MMP-2,-9 の活性について比較をおこなう。凍結肺標本より RNA を抽出し逆転写反応により cDNA を作製する。Real-time RT-PCR 法にて、elastin、collagen type3 の発現について、野生型、および FUT8 ヘテロマウス間の比較を行う。また 14 日目以後については、25cmH_2O 定圧ホルマリン固定

標本を作製し、組織学的に肺気腫の程度を比較する。動物実験については、北海道大学実験動物取り扱い委員会にて承認されており、かつ本学の実験動物指針に従う。実験の実施にあたっては、実験動物に適切な鎮痛、麻酔、保定を施し、無用の苦痛を与えないよう細心の留意を行う。

C. 結果

1:野生型マウスでは、エラスターゼ気管内投与 14 日後においては、非投与マウスに比べ、有意な気腫形成は認めない。しかし、FUT8 ヘテロマウスにおいては、すでに気腫化の形成を認め、同日の野生型と比較して肺気腫の程度に有意差を認めた。昨年度の報告に示した21日後の結果に合致するものである。本結果は、FUT8 ヘテロマウスにおいては、気腫化が早期に始まることを示唆する。

2:エラスターゼ気管内投与後の組織修復に関わる遺伝子として elastin、collagen type3 の定量をおこなった。肺組織における elastin、collagen type3 の mRNA 発現はともにエラスターゼ投与後 7 日目がピークであったが、FUT8 ヘテロマウスと野生型マウスにおいて有意差を認めなかった。

3:BAL 液中の MMP-2、MMP-9 活性を調べるため gelatin zymography をおこなった。エラスターゼ投与 24 時間後において、FUT8 ヘテロマウスでは野生型と比較して BAL 液中の pro-form、active form ともに、MMP-2 活性の有意な上昇を認めた。MMP-9 には有意な差はなかった。エラスターゼ投与 3 時間後、7 日後の BAL 液中 MMP 活性においては両群において有意な差を認めなかった。

D. 考案

FUT8(α1,6-fucosyltransferase)は糖鎖における α 1,6 フコースの結合を触媒する糖転換酵素であり、哺乳類の組織に広く分布している。FUT8 の欠損マウスでは著しい成長障害とともに、肺においては肺胞腔の拡大や肺胞壁の破壊など病理学的な肺気腫の所見を呈することが知られており、その機序として TGF-β や VEGF などの各種受容体に適切な糖鎖構造が付加されないことで受容体下流のシグナル伝達が低下することが肺気腫の形成に関与すると考えられている。今回我々は FUT8 のヘテロマウスにエラスターゼを気管内投与することで、FUT8 の完全欠損ではなく量的低下が外因性の気腫に与える影響について検討した。今回の我々の研究において FUT8 ヘテロマウスでは野生型と比較して、エラスターゼ投与による肺気腫がより早期におきること、およびエラスターゼ投与 24 時間後の BAL 液中 MMP-2 活性が上昇していることが明らかになった。

エラスターゼ気管内投与による肺気腫モデルは人間の肺気腫と生理学的・病理学的に類似した気腫様変化を喫煙曝露と比較して早期に惹起することができることから動物モデルにおいて広く用いられている。エラスターゼ投与により肺気腫が形成される機序についてはまだ完全に解明されていないが、エラスターゼ投与を契機とした各種プロテアーゼの亢進がプロテアーゼ/アンチプロテアーゼの不均衡を引き起こすことが一因とされている。今回の我々の研究でも FUT8 ヘテロマウスにおいてエラスターゼ投与 24 時間後の MMP-2 活性が上昇していた。同様の結果は FUT8 欠損マウスにおいても TGF-β 受容体の機能異常により肺組織においていくつかの MMP 発現が上昇していることが確認されている。一方で我々の昨年度の研究においては FUT8 ヘテロマウスと野生型でエラスターゼ投与後初期の好中球性炎症に差を認めなかったことから、FUT8 の量的低下は炎症の強さとは直接関係せずに MMP-2 活性の上昇に関与した可能性を考えた。今回

BAL 液中で有意に上昇していた MMP が MMP-9 ではなく、MMP-2 であったことも、炎症細胞ではなく、肺上皮細胞、線維芽細胞などの肺構成細胞、あるいはマクロファージ由来であることを示唆する。今後は FUT8 ヘテロマウスで気腫化が促進される機序のさらなる探求をおこなう予定である。

E. 結論

FUT8 ヘテロマウスを用い、エラスターゼ誘導肺気腫モデルにおいて、野生型との差を検討した。エラスターゼ投与により FUT8 ヘテロマウスでは野生型に比べてより早期に気腫が誘導された。BAL 液中の MMP-2 活性は FUT8 ヘテロマウスで野生型と比較してより亢進しており、FUT8 の量的低下が、エラスターゼ投与後の MMP 活性の上昇を介して、より早期の肺気腫形成に関与している可能性が考えられた。

F. 研究発表

1. 論文発表

1. Manicone AM, Birkland TP, Lin M, **Betsuyaku T**, van Rooijen N, Lohi J, Keski-Oja J, Wang Y, Skerrett SJ, Parks WC. Epilysin (MMP-28) restrains early macrophage recruitment in Pseudomonas aeruginosa pneumonia (2009) *J Immunol* 182, 3866-76.
2. Suzuki M, **Betsuyaku T**, Ito Y, Nagai K, Odajima N, Moriyama C, Nasuhara Y, Nishimura M. Curcumin attenuates elastase- and cigarette smoke-induced pulmonary emphysema in mice (2009) *Am J Physiol Lung Cell Mol Physiol*. In Press.
3. Onodera J, Onodera S, Kondo E, **Betsuyaku T**, Yasuda K. A soluble factor (EMMPRIN) in exudate influences knee motion after total arthroplasty (2009) *Knee Surg Sports Traumatol Arthrosc*. 17, 298-304.
4. Hasegawa M, Makita H, Nasuhara Y, Nagai K, Ito Y, Odajima N, **Betsuyaku T**, Nishimura M. Relationship between improved airflow limitation and changes in airway caliber induced by inhaled anticholinergics in chronic obstructive pulmonary disease (2008) *Thorax* 64, 332-338.
5. Nagai K, **Betsuyaku T**, Konno S, Ito Y, Nasuhara Y, Hizawa N, Kondo T, Nishimura M. Diversity of protein carbonylation in allergic airway inflammation (2008) *Free Radic Res*. 42, 921-9.
6. Odajima N, **Betsuyaku T**, Nasuhara Y, Inoue H, Seyama K, Nishimura M. Matrix metalloproteinases in blood from patients with LAM (2009) *Respir Med*. 103, 124-129.
7. Ito Y, **Betsuyaku T**, Moriyama C, Nasuhara Y, Nishimura M. Aging affects lipopolysaccharide-induced upregulation of heme oxygenase-1 in the lungs and alveolar macrophages. (2009) *Biogerontology* 10, 173-80.
8. Suzuki M, **Betsuyaku T**, Ito Y, Nagai K, Nasuhara Y, Kaga K, Kondo S, Nishimura M. Down-regulated NF-E2-related factor 2 in pulmonary macrophages of aged smokers and patients with chronic obstructive pulmonary disease (2008) *Am J Respir Cell Mol Biol*. 39, 673-82.
9. Adair-Kirk TL, Atkinson JJ, Griffin GL, Watson MA, Kelley DG, DeMello D, Senior RM, **Betsuyaku T**. Distal airways in mice exposed to cigarette smoke: Nrf2-regulated genes are increased in Clara cells (2008) *Am J Respir Cell Mol Biol*. 39, 400-411.
10. Hizawa N, Makita H, Nasuhara Y, Hasegawa M, Nagai K, Ito Y, **Betsuyaku T**, Konno S, Nishimura M; Hokkaido COPD Cohort Study Group. Functional single nucleotide polymorphisms of the CCL5 gene and nonemphysematous phenotype in COPD patients. (2008) *Eur Respir J*. 32, 372-8.

2. 学会発表

1. "Progressive infiltration of lymphocytes and upregulation of MIP-3α/CCL20 after cessation of cigarette smoke (CS) exposure in aged mice" T. Betsuyaku, C. Moriyama, Y. Ito, I. Hamamura, J. Hata, H. Takahashi, Y. Nasuhara, M. Nishimura.

American Thoracic Society 2008 International Conference, Toronto, Canada, May, 2008

G. 知的財産権の出願・登録状況

（予定を含む。）

1. 特許取得

該当なし

2. 実用新案登録

該当なし

3.その他

該当なし

研究協力者 吉田貴之（北海道大学大学院医学研究科呼吸器内科学分野大学院生）

厚生労働科学研究費補助金（創薬基盤推進研究事業）

分担研究報告書

マウスにおける環境因子曝露とFut8活性の肺気腫変化に及ぼす影響の解析

分担研究者　前野　敏孝　群馬大学大学院医学系研究科　臓器病態内科学

研究要旨：糖転移酵素 Fut8 ノックアウトマウスにおいて肺気腫様の変化が認められる．我々はこれまでに，肺気腫の主要な原因である喫煙による Fut8 活性の変化をマウスへの喫煙実験を用いて解析し，Fut8 活性が野生型および Fut8 ヘテロ欠損マウスいずれにおいても、喫煙後に有意な活性の低下を示すことを明らかにした。さらに，肺気腫の指標である平均肺胞径が Fut8+/-で喫煙後に有意に増加を示し，Fut8 ヘテロ欠損マウスへの喫煙曝露モデルは，早期肺気腫発症モデルと位置付けられることを明らかにした。

平成20年度は，Fut8ヘテロ欠損マウスにおける喫煙による肺気腫発症の分子機序解明のため，MMP活性の検討を行った。 2週間の喫煙曝露によりFut8ヘテロ欠損マウスにおけるMMP-9・12・13活性が有意に上昇し，4週以上の曝露ではMMP活性の上昇は消失していた。 Fut8活性の低下しているFut8ヘテロ欠損マウスでは，喫煙曝露によりMMP活性が上昇し，肺胞が破壊され，肺気腫が形成されるものと考えられる。 本マウスは，MMP阻害活性を有する薬剤など，新規COPD治療候補薬の評価において有意義なモデルである。

A. 研究目的

慢性閉塞性肺疾患（COPD）はタバコなどの有毒な粒子やガスの吸入によって生じた，肺の炎症反応に基づく進行性の気流制限を呈する疾患である。 現在，世界の死亡原因の第 4 位となっており，本疾患は世界的に重大な問題である。 日本においても 40 歳以上の男性の 16.4%，女性の 5.0%，全体の 8.6%という高い有病率（530 万人）であることが明らかになってきた。 現在の COPD の治療は，禁煙・気管支拡張剤の投与が中心である。 病因としては，1）プロテアーゼ・アンチプロテアーゼ不均衡　2）オキシダント・アンチオキシダント不均衡などが考えられ，その意義が検討されてきたが，プロテアーゼやオキシダントをターゲットとした治療法は確立されておらず，新たな機序で COPD の病態を抑制できる治療薬の開発が強く求められている。

糖鎖の機能解析の研究において，N 型糖鎖にコアフコースが付加（α1，6 フコシル化）されると，そのターゲットタンパク質の機能が変化すること，またコアフコシル化を触媒する Fut8（α1,6 fucosyltransferase）の遺伝子欠損マウス（ノックアウトマウス）は，著明な成長障害と肺気腫様病変を示すことを明らかにしてきた。

この肺気腫様病変は，TGFβ 受容体に対するコアフ

コースの付加がなされないため，TGFβ受容体の下流シグナルが減弱し抑制系に働くSmadのリン酸化が十分に起こらなくなることから細胞外マトリックスの分解を主につかさどるマトリックスメタロプロテアーゼ(MMP)の遺伝子発現が高まり，肺胞壁の合成と分解のバランスが崩れることにより肺気腫様の病変が引き起こされることを明らかにした．この研究により，糖鎖異常が肺気腫の原因になる可能性を示した。

さらに，野生型とほぼ同じ生存を示し Fut8 活性が野生型に比較して約半分に減弱しているヘテロノックアウトマウス(Fut8+/-)を用いて喫煙曝露を行い，喫煙によるFut8 活性の変化を解析した．Fut8 活性は野生型およびFut8+/-いずれにおいても，喫煙後に有意な活性の低下を示し，さらに，肺気腫の指標である平均肺胞径がFut8+/-で喫煙後に有意に増加を示し，Fut8+/-への喫煙曝露モデルは，早期肺気腫発症モデルと位置付けられることを明らかにした。

平成 20 年度は，Fut8 ヘテロ欠損マウスにおける喫煙による肺気腫発症の再現性を確認すると共に，分子機序解明のため，MMP 活性の検討を行った。

B. 研究方法

1．マウスにおける喫煙曝露

野生型マウスおよびFut8+/-マウスを用いて，喫煙曝露を行った。 喫煙曝露は，1日4本を週6日施行した．タバコはケンタッキー大学のResearch Cigarette(2R4F)を使用した。 1日4本，週6日，3ヶ月間の喫煙曝露を行喫煙終了翌日に，右肺を25cmH2O圧にて10分間ホルマリン固定した。 固定した肺は，24時間固定後，包埋しH.E.標本を作製した。 このH.E.標本を用いて，肺胞径を測定し，平均肺胞径を算出した。

2．MMP活性の測定

トータル活性

(1)各サンプルを分子量三万カットの遠心式限外濾過ユニットで TIMP や細胞外マトリックス由来の低分子量物質などの阻害物質を除去する。

(2)10μg のタンパク質を酵素源として用いた蛍光基質{DNP-Pro-Cha-Gly-Cys(Me)-His-Ala-Lys(N-Me-Abz)-NH2 [Cha = B-cyclohexylalanyl; Abz = 2-aminobenzoyl (anthraniloyl)]を最終濃度 4μM の条件下で使用した。この基質は MMP により分解されると蛍光(Ex. 365nm, Em.450 nm)を発するため，分解産物量を経時的に測定した。

MMP-9, MMP-13 の定量

(1)抗体プレートを用いて各サンプル 100μg にある MMP-9 または MMP-13 を吸着させる。

(2)ELISA と同様に，洗浄後，蛍光基質と反応させ，検出を行った。

MMP-12 の相対活性

(1)各サンプルを分子量三万カットの遠心式限外濾過ユニットで TIMP や細胞外マトリックス由来の低分子量物質などの阻害物質を除去する。

(2)基質と反応する前に，MMP-12 の inhibitor 1μl(最終濃度 80nM)を溶液に加え，各サンプルと pre-incubation する(37℃, 30 分)。

(3) 10μg のタンパク質を酵素源として用いた．蛍光基質{DNP-Pro-Cha-Gly-Cys(Me)-His-Ala-Lys(N-Me-Abz)-NH2 [Cha = B-cyclohexylalanyl; Abz = 2-aminobenzoyl (anthraniloyl)]を最終濃度 4μM の条件下で使用した．この基質は MMP により分解されると蛍光(Ex. 365nm, Em.450 nm)を発するため，分解産物量を経時的に測定した。

(4)阻害剤の有無による活性の差を MMP-12 活性とした．つまり，[(阻害剤なし－阻害剤あり)/阻害剤なし

X100%]として算出した。

(MMP 活性は代表研究者の所属機関である大阪大学疾患糖鎖学の高 晨笑先生に測定いただきました)

(倫理面への配慮)

動物実験に関しては,「厚生労働省の所管する実施機関における動物実験等の実施に関する基本指針」ならびに「動物実験の適正な実施に向けたガイドライン」を尊守して作成された実験計画により実施している。

C. 研究結果

1. Fut8ヘテロ欠損マウスにおける喫煙曝露, その後の平均肺胞径の変化を検討した。 平均肺胞径は, 野生型では非喫煙群33.02±2.52, 喫煙群36.25±3.02と有意な変化は認めなかった。 一方, Fut8+/-においては, 非喫煙群34.31±2.48, 喫煙群40.1±1.58と再現性を持って, 有意な平均肺胞径の増加を認めた。

2. MMP 活性の測定

2 週間の喫煙曝露により, Fut8+/-マウスにおける MMP-9 活性および MMP-13 活性が有意に上昇した。 MMP-12 の相対活性も有意な上昇が認められた。 野生型では喫煙後も有意な上昇は認めなかった。Total の MMP 活性では有意差は認められなかった (Fig 1)。

この MMP 活性の変化を経時的に検討したところ, 2 週曝露において認められた MMP-9 活性, MMP-13 活性および MMP-12 の相対活性の上昇は, 4 週曝露以降は有意差が認められなくなった(Fig 2)。

D. 考察

従来、喫煙曝露による肺気腫のモデルマウスの作成には6ヶ月間を要すると考えられてきた。 今回の我々の検討により, Fut8+/-への喫煙曝露モデルは, 3ヶ月という従来よりも短縮した期間で再現性を持って肺気腫を作成できる。 早期肺気腫発症モデルと位置付けることができる。

また, 本モデルは, 喫煙曝露早期に MMP-9・MMP-12・MMP-13 活性が増加し, 肺胞が破壊されることで, 肺気腫が形成されると考えられた。 今後, Fut8+/-への喫煙曝露モデルを用いた, MMP 阻害剤の効果の検討などが重要と考えられる。

E. 結論

Fut8+/-への喫煙曝露モデルは, 3ヶ月という従来よりも短縮した期間で肺気腫を作成できる。 早期肺気腫発症モデルと位置付けることができる。 肺気腫発症のメカニズムとして, 喫煙曝露早期のMMP-9・MMP-12・MMP-13の増加が示唆された。

このFut8+/-への喫煙曝露モデルは, 今後のCOPD治療候補薬の評価などにおいて, 大変有意義なモデルと考えられる。

F. 研究発表

1. 論文発表

該当なし

2. 学会発表

該当なし

G. 知的財産権の出願・登録状況(予定を含む。)

1. 特許取得

該当なし

2. 実用新案登録

該当なし

3.その他

該当なし

Figure 1.　2週間喫煙曝露マウスのMMP活性変化

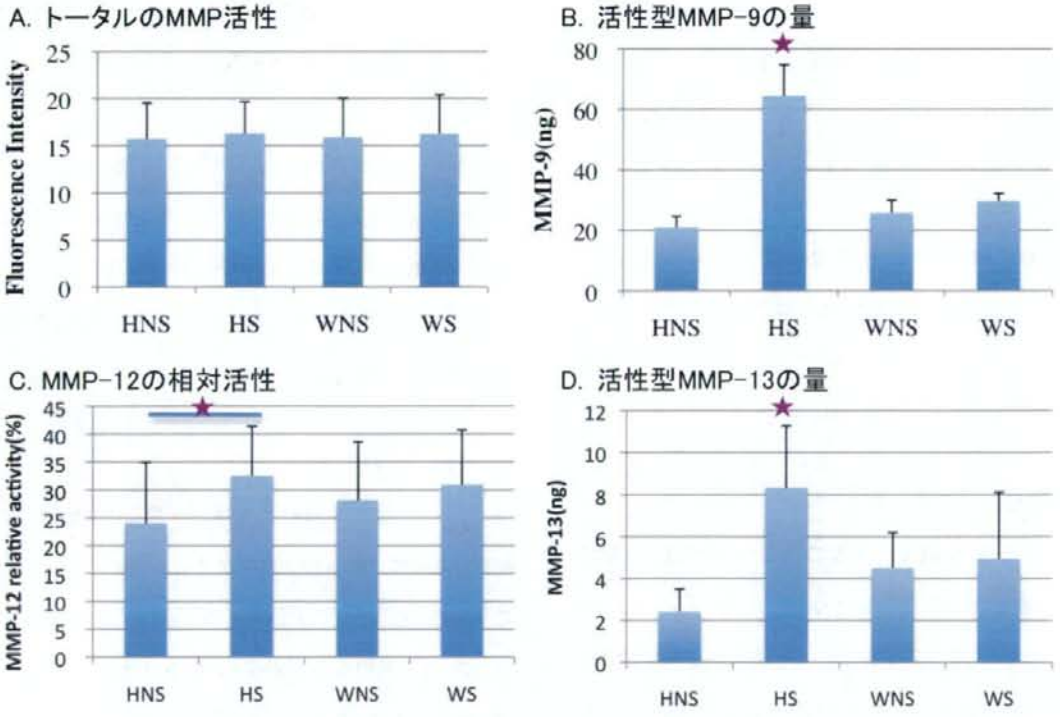

Figure 2.　喫煙曝露マウスにおけるMMP活性の経時的変化

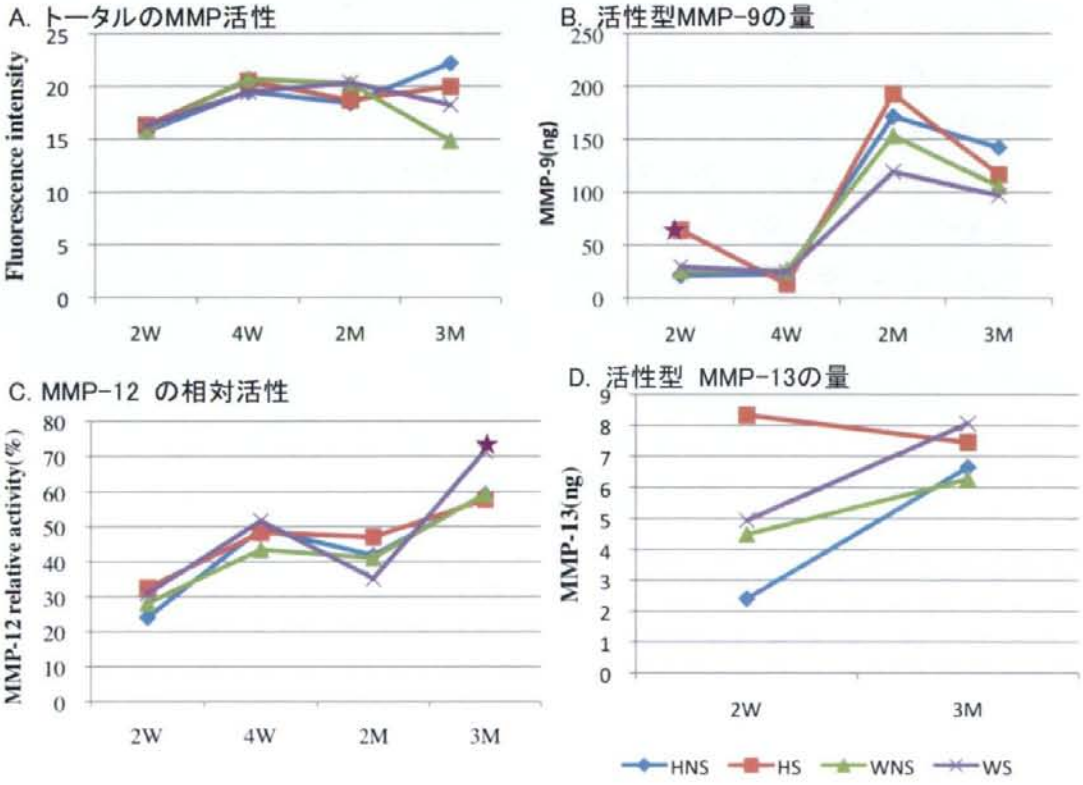

研究成果の刊行に関する一覧表

著書

無し

雑誌

発表者氏名	論文タイトル名	発表誌名	巻号	ページ	出版年
S. Kitazume, R. Oka, K. Ogawa, S. Futakawa, Y. Hagiwara, H. Takigawa, M. Kato, A. Kasahara, E. Miyoshi, N. Taniguchi, and Y. Hashimoto.	Molecular insights into {beta}-galactoside {alpha}2,6-sialyltransferase secretion in vivo.	Glycobiology	19	479-487	2009
M. Nakano, D. Higo, E. Arai, T. Nakagawa, K. Kakehi, N. Taniguchi, and A. Kondo	Capillary electrophoresis-electrospray ionization mass spectrometry for rapid and sensitive *N*-glycan analysis of glycoproteins as 9-fluorenylmethyl derivatives.	Glycobiology	19	135-143	2009
T. Okada, H. Ihara, R. Ito, N. Taniguchi, and Y. Ikeda.	Bidirectional *N*-acetylglucosamine transfer mediated by beta-1,4-*N*-acetylglucosaminyltransferase III.	Glycobiology	19	368-374	2009
X. Wang, T. Fukuda, W. Li, C. X. Gao, A. Kondo, A. Matsumoto, E. Miyoshi, N. Taniguchi, and J. Gu	Requirement of Fut8 for the expression of vascular endothelial growth factor receptor-2: a new mechanism for the emphysema-like changes observed in Fut8-deficient mice.	J. Biochem.		In Press	2009
J. Gu, Y. Sato, Y. Kariya, T. Isaji, N. Taniguchi, and T. Fukuda.	A mutual regulation between cell-cell adhesion and *N*-glycosylation: implication of the bisecting GlcNAc for biological functions.	J. Proteome Res.	8	431-435	2009
T. Suzuki, I. Matsuo, K. Totani, S. Funayama, J. Seino, N. Taniguchi, Y. Ito, and S. Hase	Dual-gradient high-performance liquid chromatography for identification of cytosolic high-mannose-type free glycans.	Anal. Biochem.	381	224-232	2008
H. Inohara, T. Segawa, A. Miyauchi, T. Yoshii, S. Nakahara, A. Raz, M. Maeda, E. Miyoshi, N. Kinoshita, H. Yoshida, M. Furukawa, Y. Takenaka, Y. Takamura, Y. Ito, and N. Taniguchi.	Cytoplasmic and serum galectin-3 in diagnosis of thyroid malignancies.	Biochem. Biophys. Res. Commun.	376	605-610	2008
J. Gu, and N. Taniguchi.	Potential of *N*-glycan in cell adhesion and migration as either a positive or negative regulator.	Cell Adh. Migr.	2	243-245	2008
T. Kizaki, T. Izawa, T. Sakurai, S. Haga, N. Taniguchi, H. Tajiri, K. Watanabe, N. K. Day, K. Toba, and H. Ohno.	beta(2)-Adrenergic receptor regulates Toll-like receptor-4-induced nuclear factor-kappaB activation through beta-arrestin 2.	Immunology	124	348-356	2008
T. Nakagawa, E. Miyoshi, T. Yakushijin, N. Hiramatsu, T. Igura, N. Hayashi, N. Taniguchi, and A. Kondo.	Glycomic analysis of alpha-fetoprotein L3 in hepatoma cell lines and hepatocellular carcinoma patients.	J. Proteome Res.	7	2222-2233	2008
Y. S. Kim, S. Y. Hwang, H. Y. Kang, H. Sohn, S. Oh, J. Y. Kim, J. S. Yoo, Y. H. Kim, C. H. Kim, J. H. Jeon, J. M. Lee, H. A. Kang, E. Miyoshi, N. Taniguchi, H. S. Yoo, and J.	Functional proteomics study reveals that *N*-Acetylglucosaminyltransferase V reinforces the invasive/metastatic potential of colon cancer through aberrant glycosylation on tissue inhibitor of metalloproteinase-1.	Mol. Cell Proteomics.	7	1-14	2008

H. Ko.					
R. Akama, Y. Sato, Y. Kariya, T. Isaji, T. Fukuda, L. Lu, N. Taniguchi, M. Ozawa, and J. Gu.	*N*-acetylglucosaminyltransferase III expression is regulated by cell-cell adhesion via the *E*-cadherin-catenin-actin complex.	Proteomics	8	3221-3228	2008
Y. S. Kim, O. L. Son, J. Y. Lee, S. H. Kim, S. Oh, Y. S. Lee, C. H. Kim, J. S. Yoo, J. H. Lee, E. Miyoshi, N. Taniguchi, S. M. Hanash, H. S. Yoo, and J. H. Ko.	Lectin precipitation using phytohemagglutinin-L(4) coupled to avidin-agarose for serological biomarker discovery in colorectal cancer..	Proteomics	8	3229-3235	2008
Isaji, T., Sato, Y., Fukuda,T. and Gu, J.	N-glycosylation of the I-like domain of beta1 integrin is essential for beta1 integrin expression and biological function: Identification of the minimal N-glycosylation requirement for alpha 5beta 1.	J. Biol. Chem.		In press	2009
Sato, Y., Isaji, T., Tajiri, M., Yoshida-Yamamoto, S., Yoshinaka, T., Somehara, T., Fukuda, T., Wada, Y. and Gu, J.	An N-glycosylation site on the beta-propeller domain of the integrin alpha5 subunit plays key roles in both its function and site-specific modification by beta 1,4-N-acetylglucosaminyltransferase III.	J. Biol. Chem.		In press	2009
Manicone AM, Birkland TP, Lin M, Betsuyaku T, van Rooijen N, Lohi J, Keski-Oja J, Wang Y, Skerrett SJ, Parks WC.	Epilysin (MMP-28) restrains early macrophage recruitment in Pseudomonas aeruginosa pneumonia.	J Immunol.	182	3866-76	2009
Suzuki M, Betsuyaku T, Ito Y, Nagai K, Odajima N, Moriyama C, Nasuhara Y, Nishimura M	Curcumin attenuates elastase- and cigarette smoke-induced pulmonary emphysema in mice.	Am J Physiol Lung Cell Mol Physiol.	296	L614-623	2009
Onodera J, Onodera S, Kondo E, Betsuyaku T, Yasuda K	A soluble factor (EMMPRIN) in exudate influences knee motion after total arthroplasty.	Knee Surg Sports Traumatol Arthrosc.	17	298-304	2009
Hasegawa M, Makita H, Nasuhara Y, Nagai K, Ito Y, Odajima N, Betsuyaku T, Nishimura M	Relationship between improved airflow limitation and changes in airway caliber induced by inhaled anticholinergics in chronic obstructive pulmonary disease.	Thorax	64	332-338	2008
Nagai K, Betsuyaku T, Konno S, Ito Y, Nasuhara Y, Hizawa N, Kondo T, Nishimura M.	Diversity of protein carbonylation in allergic airway inflammation.	Free Radic Res.	42	921-929	2008
Odajima N, Betsuyaku T, Nasuhara Y, Inoue H, Seyama K, Nishimura M	Matrix metalloproteinases in blood from patients with LAM.	Respir Med.	103	124-129	2009
Ito Y, Betsuyaku T, Moriyama C, Nasuhara Y, Nishimura M.	Aging affects lipopolysaccharide-induced upregulation of heme oxygenase-1 in the lungs and alveolar macrophages.	Biogerontology	10	173-80	2009
Suzuki M, Betsuyaku T, Ito Y, Nagai K, Nasuhara Y, Kaga K, Kondo S, Nishimura M.	Down-regulated NF-E2-related factor 2 in pulmonary macrophages of aged smokers and patients with chronic obstructive pulmonary disease.	Am J Respir Cell Mol Biol.	39	673-682	2008
Hizawa N, Makita H, Nasuhara Y, Hasegawa M, Nagai K, Ito Y, Betsuyaku T, Konno S, Nishimura M; Hokkaido COPD Cohort Study Group.	Functional single nucleotide polymorphisms of the CCL5 gene and nonemphysematous phenotype in COPD patients.	Eur Respir J.	32	372-378	2008

Glycobiology vol. 19 no. 5 pp. 479–487, 2009
doi:10.1093/glycob/cwp003
Advance Access publication on January 15, 2009

Molecular insights into β-galactoside α2,6-sialyltransferase secretion in vivo

Shinobu Kitazume[1,2,4,5], Ritsuko Oka[4,5], Kazuko Ogawa[4,5], Satoshi Futakawa[3,4,5], Yoshiaki Hagiwara[6], Hajime Takikawa[7], Michio Kato[8], Akinori Kasahara[9], Eiji Miyoshi[10], Naoyuki Taniguchi[2,11], and Yasuhiro Hashimoto[3,4,5]

[4]Glyco-chain Functions Laboratory, RIKEN, 2-1 Hirosawa, Wako-shi, Saitama 351-0198; [5]CREST, Japan Science and Technology Agency, Kawaguchi, Saitama 560-0082; [6]Department of Biological Sciences, Immuno-Biological Laboratories, 1091-1 Naka, Fujioka-shi, Gunma 375-0005; [7]Department of Medicine, Teikyo University School of Medicine, Kaga 2-11-1, Itabashi, Tokyo 173-8605; [8]Department of Gastroenterology, Osaka National Hospital, 2-1-14, Ho-enzaka, Chu-oku, Osaka 540-0006; [9]Department of General Medicine, 2-2 Yamada-oka, Suita; [10]Department of Molecular Biochemistry and Clinical Investigation; and [11]Department of Biochemistry, Osaka University Graduate School of Medicine, 1-7, Yamada-Oka, Osaka 565-0871, Japan

Received on November 12, 2008; revised on December 15, 2008; accepted on January 6, 2009

β-Galactoside α2,6-sialyltransferase (ST6Gal I), which is highly expressed in the liver, is mainly cleaved by Alzheimer's β-site amyloid precursor protein-cleaving enzyme 1 (BACE1) and secreted into the serum. During our studies to elucidate the molecular mechanism underlying the cleavage and secretion of ST6Gal I, we hypothesized that plasma ST6Gal I may represent a sensitive biomarker for hepatopathological situations. In the present study, we used recently developed sandwich ELISA systems that specifically detect the soluble cleaved form of ST6Gal I in plasma. We found that the level of plasma ST6Gal I was increased in two different types of liver injury models. In zone 1 hepatocyte-injured rats, the level of plasma ST6Gal I was increased together with acute phase reactions. Meanwhile, in zone 3 hepatocyte-injured rats, ST6Gal I secretion was most likely triggered by oxidative stress. Taken together, we propose two possible mechanisms for the upregulation of plasma ST6Gal I in hepatopathological situations: one accompanied by acute phase reactions to increase hepatic ST6Gal I expression and the other triggered by oxidative stress in the liver. We also found that the serum level of ST6Gal I in hepatitis C patients was correlated with the activity of hepatic inflammation.

Keywords: acute phase reaction/BACE1/hepatitis/secretion/ST6Gal I

Introduction

Sialic acid (Sia) molecules attached to glycoproteins or glycosphingolipids play important roles in many biological processes, including immune recognition, binding of pathogens to host cells, and cell adhesion and apoptosis (Varki 1999). Sialyltransferases are key enzymes that regulate the cellular levels of Sia-containing molecules. β-Galactoside α2,6-sialyltransferase (ST6Gal I), which catalyzes α2,6-sialylation of Galβ1,4-GlcNAc structures on *N*-glycans, is a type-II membrane protein localized in the trans-Golgi network (Weinstein et al. 1987; Colley et al. 1992). ST6Gal I is highly expressed in the liver and also expressed in most other tissues to some extent (Kitagawa and Paulson 1994). ST6Gal I deficiency causes abnormalities in B-cell immunoreactivity (Hennet et al. 1998), which can be partly explained by a recent report showing that ST6Gal I deficiency induces IgM antigen receptor endocytosis in the absence of immune stimulation (Collins et al. 2006; Grewal et al. 2006). The expression and activity of ST6Gal I are often discussed in association with tumor metastasis in breast (Recchi et al. 1998) and colon (Dall'Olio et al. 2001) cancers. The cellular level of ST6Gal I in cancer cells influences the sialylation of integrins, thereby affecting their binding affinities for fibronectin (Semel et al. 2002). Similar to the case for some glycosyltransferases, the majority of ST6Gal I in the liver is cleaved and secreted into the serum (Weinstein et al. 1987; Colley et al. 1989). We previously demonstrated that the predominant protease involved in this cleavage and secretion of ST6Gal I is the β-site amyloid precursor protein (APP)-cleaving enzyme 1 (BACE1) (Kitazume et al. 2001, 2003, 2005), which cleaves APP to produce the neurotoxic amyloid β-peptide (Aβ) and has been implicated in triggering the pathogenesis of Alzheimer's disease (Hussain et al. 1999; Sinha et al. 1999; Vassar et al. 1999; Yan et al. 1999; Bennett et al. 2000). We recently showed that ST6Gal I cleavage by BACE enhances the sialylation of soluble glycoproteins (Sugimoto et al. 2007). Previous studies have shown that plasma ST6Gal I activity is upregulated in particular hepatopathological situations. First, turpentine-injected mice exhibited physiological changes, designated hepatic acute phase reactions, such as increased synthesis of serum glycoproteins together with enhanced plasma ST6Gal I secretion, indicating that plasma ST6Gal I is one of the acute phase reactants (Kaplan et al. 1983; Dalziel et al. 1999). Second, our recent study using Long-Evans Cinnamon (LEC) rats, which spontaneously accumulate copper in their liver due to a genetic mutation in copper-transporting ATPase (ATP7B) and incur hepatic damage (Mori et al. 1991; Suzuki et al. 1993; Wu et al. 1994), revealed that LEC rats showed increases in soluble ST6Gal I in the plasma much earlier than the development of hepatitis (Kitazume et al. 2005). Generation of intracellular soluble ST6Gal I would be related to effective sialylation of plasma glycoproteins (Sugimoto et al. 2007), thereby avoiding the clearance of these glycoproteins by

[1]To whom correspondence should be addressed: Tel: +81-48-467-9616; Fax: +81-48-467-9617; e-mail: shinobuk@riken.jp
[2]Present address: Disease Glycomics Team, RIKEN Advanced Science Institute, 2-1 Hirosawa, Wako-shi, Saitama 351-0198, Japan.
[3]Present address: School of Medicine, Department of Biochemistry, Fukushima Medical University, Hikarigaoka-1, Fukushima-shi, Fukushima 960-1295, Japan.

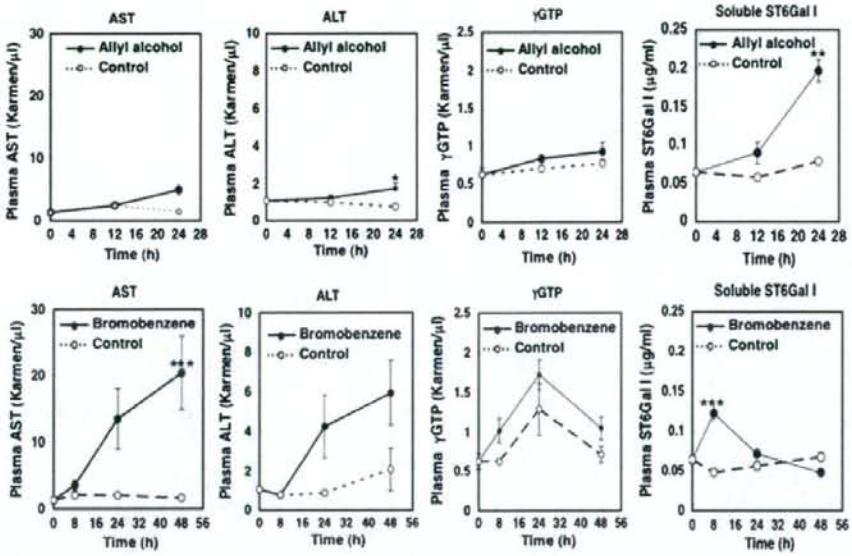

Fig. 1. Soluble ST6Gal I and hepatitis marker levels in zone 1 or zone 3 hepatocyte-injured rats. After AA or BB administration to elicit zone 1 or zone 3 hepatocyte injury, respectively, rat plasma samples were analyzed for their levels of soluble ST6Gal I and the hepatitis marker enzymes γ-GTP, AST, and ALT. Data represent the mean ± SEM ($n = 4$). $^{*}P < 0.05$; $^{**}P < 0.002$; $^{***}P < 0.005$.

hepatic asialoglycoprotein receptors. Another hypothesis is that plasma ST6Gal I may be a sensitive biomarker for diagnosing hepatological inflammation. Currently, the most effective strategy for decreasing hepatocellular carcinoma-related mortality is early detection (Bruix et al. 2004).

In the present study, we used two recently developed sandwich ELISA systems for quantifying plasma ST6Gal I (Futakawa et al. 2009). We initially applied these ELISA systems to two different types of chemically induced rat hepatitis models involving selective injuries to zone 1 hepatocytes in periportal areas and zone 3 hepatocytes located near the central vein, respectively (Aiso et al. 2000). We further describe two distinct underlying mechanisms for stimulating ST6Gal I secretion in these different liver injury systems. We subsequently used the ELISA systems to measure the serum levels of ST6Gal I in hepatitis patients.

Results

ST6Gal I sandwich ELISA systems

In the present study, we used two kinds of recently developed sandwich ELISA systems I (Futakawa et al. 2009) to detect plasma ST6Gal I. We previously showed that the majority of the rat ST6Gal I secreted by cells started at $E^{41}F^{42}Q^{43}$ (E41 form) (Kitazume-Kawaguchi et al. 1999; Kitazume et al. 2001). In the α2,6-sialyltransferase (E41 form) sandwich ELISA system for detecting plasma/serum ST6Gal I in rats, we prepared an anti-ST6Gal I E41 antibody that specifically recognized the E41 form of rat ST6Gal I. For the quantification of plasma/serum ST6Gal I in other species, we subsequently developed an α2,6-sialyltransferase (M2) ELISA system using an anti-ST6Gal I M2 antibody obtained by immunization with KLH-NSQLVTTEKRFLKDSL, a common sequence in rat, mouse, and human ST6Gal I. When we performed E41 ELISA and M2 ELISA for rat plasma, the obtained results were almost indistinguishable (Futakawa et al. 2009). The linear range of the M2 ELISA was 1–70 ng/mL while that of the E41 ELISA was 0.3–20 ng/mL.

Zone 1 hepatocyte-injured rats

Previous studies have shown that plasma ST6Gal I is upregulated in particular hepatopathological situations (Kaplan et al. 1983; Dalziel et al. 1999; Kitazume et al. 2005). Here, we employed two kinds of established experimental liver injury models to examine the changes in the plasma ST6Gal I levels. First, we established zone 1 hepatocyte-injured rats by administering AA and measured their plasma levels of ST6Gal I. AA administration induces marked periportal (zone 1) hepatocellular necrosis (Aiso et al. 2000). Although low doses of AA did not increase the levels of hepatitis markers such as ALT, AST, and γ-GTP (Figure 1, upper panels), a significant increase in plasma ST6Gal I was detected at 12 h after AA administration. At 24 h after AA administration, the level of plasma ST6Gal I showed an ~3-fold elevation. To examine whether hepatic acute phase reactions occurred in AA-injected rats, we measured the plasma levels of acute phase reactants. As shown in Figure 2, the levels of both α2-macroglobulin and haptoglobin were markedly increased, indicating the presence of hepatic acute phase reactions. In turpentine-injected mice, the hepatic acute phase responses are paralleled by an increase in hepatic ST6Gal I expression (Dalziel et al. 1999). In our previous study using hepatitis model LEC rats, increased BACE1 expression coincided with elevation of plasma ST6Gal I (Kitazume et al.

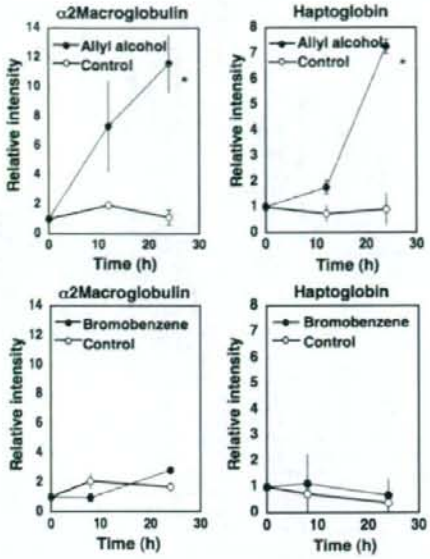

Fig. 2. Levels of acute phase plasma proteins in chemically induced hepatitis models. After zone 1 or zone 3 hepatocyte injury, rat plasma samples were analyzed for their levels of α2-macroglobulin (10 μg of plasma protein) and haptoglobin (1 μg of plasma protein) by Western blotting. Data represent the mean ± SEM ($n = 4$). All values were normalized by the corresponding level in control rats. $^*P < 0.05$.

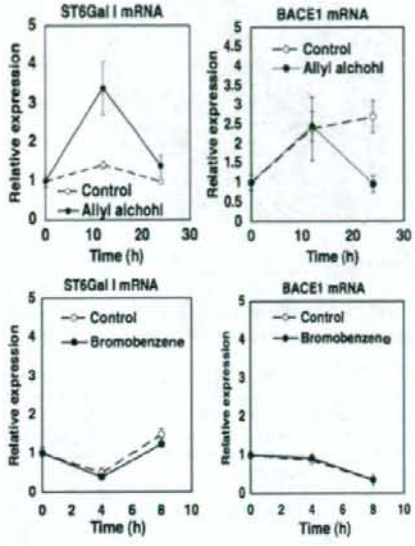

Fig. 3. Changes in the expression levels of ST6Gal I and BACE1 in zone 1 or zone 3 hepatocyte-injured rats. Total RNA was isolated from liver tissues of zone 1 or zone 3 hepatocyte-injured rats and control rats. The amounts of BACE1 and GAPDH mRNAs in the livers were analyzed by real-time PCR using a standard curve method. The amounts of ST6Gal I mRNA relative to GAPDH mRNA were determined by the comparative C_T method. All data represent the mean ± SEM ($n = 3$).

2005). Therefore, we subsequently analyzed the expression levels of liver ST6Gal I and BACE1. As shown in Figure 3 (upper panels), zone 1 hepatocyte-injured rats showed an ~3-fold elevation of hepatic ST6Gal I mRNA by 12 h after AA administration. In contrast, the level of hepatic BACE1 mRNA was increased in both AA-injected and PBS-injected control rats for unknown reason. ST6Gal I expression is regulated by multiple independent promoters (Wuensch et al. 2000). Lau's group has beautifully showed that elevation of hepatic and serum ST6Gal I as a result of acute phase reaction is governed by the inducible, liver-specific promoter, P1 (Appenheimer et al. 2003). Taken together, these results strongly suggest that the elevation of plasma ST6Gal I following zone 1 hepatocyte injury is due to an increase in hepatic ST6Gal I expression.

Zone 3 hepatocyte-injured rats

Next, we examined whether plasma ST6Gal I is elevated in zone 3 hepatocyte-injured rats by administering BB. BB administration produces hepatocellular necrosis near the central vein (zone 3) with attendant inflammation (Aiso et al. 2000). At 24 h after BB administration, we observed significant increases in plasma ALT and AST (Figure 1, lower panels). Although plasma γ-GTP was also slightly increased at 8 h and 24 h after BB administration, control mice showed similar increases, indicating that BB itself did not elicit γ-GTP elevation. Interestingly, the elevation of plasma ST6Gal I was much faster, occurring at 8 h after the BB injection. Since the levels of plasma α2-macroglobulin and haptoglobin were not increased (Figure 2, lower panels), acute phase reactions were not elicited by BB administration. In contrast to the case for zone 1 hepatocyte injury, the expression levels of both ST6Gal I and BACE1 in the liver remained unchanged (Figure 3, lower panels). These data indicate that the increase in plasma ST6Gal I following zone 3 hepatocyte injury is mediated by a different molecular mechanism from that following zone 1 hepatocyte injury.

Oxidative stress occurs in zone 3 hepatocyte-injured rats

The mechanism and toxicity of BB have previously been described in detail (Lau and Monks 1988). In the liver, BB is subjected to epoxidation as a result of biotransformation to enable its excretion in the urine, followed by conjugation to glutathione, thereby leading to depletion of hepatic cellular glutathione and elicitation of oxidative stress (Heijne et al. 2003). We therefore hypothesized that oxidative stress induced in the liver could be a trigger for plasma ST6Gal I secretion. Initially, we analyzed whether proteins responding to oxidative stress were actually increased in the liver at 8 h after BB administration. As shown in Figure 4A (lower panels), 4-HNE, a lipid peroxide end product, was increased in the plasma membrane of hepatic cells near the central vein at 8 h after BB administration, even though no significant differences were observed between the hematoxylin and eosin staining patterns for BB-injected and control livers (Figure 4A, upper panels). It seems that this 4-HNE increase is locally restricted, as we failed to detect a significant increase in lipid peroxidation indicators (e.g., plasma hexanoyl-lysine adduct and malondialdehyde in livers)

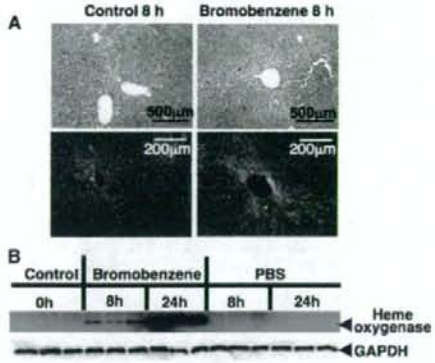

Fig. 4. Oxidative marker proteins in the liver of zone 3 hepatocyte-injured rats. (**A**) At 8 h after bromobenzene administration, rat liver tissues were removed and processed for the preparation of paraffin-embedded sections. After deparaffinization, the sections were stained with hematoxylin and eosin (upper panels) or immunostained with an anti-4-HNE antibody (lower panels). (**B**) After bromobenzene administration, rat liver tissues were removed and homogenized. Liver homogenates (10 μg of protein) were analyzed by Western blotting using anti-heme oxygenase and anti-GAPDH antibodies.

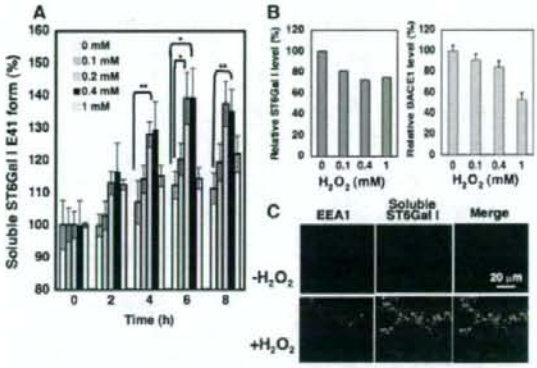

Fig. 5. Effects of H_2O_2 on the secretion of ST6Gal I by rat hepatocytes. Rat hepatocytes grown on collagen-type I-coated plates (60 mm) were treated with H_2O_2 (0, 0.1, 0.2, 0.4, or 1 mM) for 0, 2, 4, 6, or 8 h. (**A**) At each time point, 100 μL of the medium was removed and analyzed using the α2,6-sialyltransferase (E41 form) sandwich ELISA kit. All data represent the mean ± SEM ($n = 3$). $^*P < 0.02$; $^{**}P < 0.05$. (**B**) At 6 h after the H_2O_2 addition (0, 0.1, 0.4, or 1 mM), cell lysates were prepared for analyses of intact ST6Gal I or BACE1 using appropriate sandwich ELISA kits. The data for BACE1 represent the mean percentages of these proteins ± SEM ($n = 3$). (**C**) Rat hepatocytes were grown on collagen-type I-coated chamber slides at 33°C to allow the accumulation of newly synthesized material in the trans-Golgi network, and then treated with 0.4 mM H_2O_2 for 1 h. After methanol fixation, the cells were incubated with anti-ST6Gal I E41 and anti-EEA1 antibodies, followed by Alexa Fluor 488-conjugated anti-rabbit IgG and Alexa Fluor 546-conjugated anti-mouse IgG.

after BB administration (data not shown). Heme oxygenase-1, a protein induced by the oxidative stress response, was increased in the zone 3 hepatocyte-injured liver (Figure 4B). The significant increase in the heme oxygenase level in the liver at 24 h after BB injection could be due to the emigration of leukocytes, in which heme oxygenase is induced as a consequence of the inflammatory response (Bussolati et al. 2004).

Oxidative stress induces ST6Gal I secretion by hepatocytes

Next, we investigated whether oxidative stress could directly induce hepatic ST6Gal I secretion into the plasma. To address this issue, hepatocytes isolated from rat livers were incubated in the presence or absence of H_2O_2, and the soluble ST6Gal I levels in the media were quantitatively analyzed at regular time intervals. At 4 h and 6 h after the addition of 0.2 or 0.4 mM H_2O_2, significant increases in soluble ST6Gal I were observed (Figure 5A), indicating that ST6Gal I secretion responded to oxidative stress. We further analyzed the levels of intact ST6Gal I in hepatocytes following H_2O_2 treatment, but found that the levels of both ST6Gal I and BACE1 were rather decreased upon H_2O_2 stimulation (Figure 5B). The increase in soluble ST6Gal I in response to H_2O_2 was only observed in primary hepatocyte cells that had been freshly prepared and was not found in either hepatocytes that had been cultured in a 5% CO_2 incubator for a longer period or in established cultures of cells such as Hep3B and HEK-ST6Gal I (supplementary Figure S1), possibly because these cells have been already exposed to an oxidative environment. We further analyzed the intracellular soluble ST6Gal I in hepatocytes using confocal fluorescence microscopy. Although we were unable to detect the soluble ST6Gal I E41 form in control hepatocytes, we did detect ST6Gal I E41 around the perinuclear area in cells treated with 0.1–1 mM H_2O_2 (Figure 5C), again confirming our observation that oxidative stress induces ST6Gal I secretion from hepatocytes.

Oxidative stress changes the intracellular localizations of ST6Gal I and BACE1

Based on our observations that the H_2O_2 addition neither increased the cellular levels of BACE1 nor activated BACE1 activity in vitro (data not shown), we hypothesized that oxidative treatment would change the subcellular localizations of ST6Gal I and/or BACE1 in such a way that a greater number of ST6Gal I substrate molecules would be in the same intracellular membrane compartment as BACE1 protease molecules. We therefore analyzed the subcellular localizations of ST6Gal I and BACE1 using confocal fluorescence microscopy (Figure 6A). Both exogenous and endogenous ST6Gal I were localized to the perinuclear Golgi region in Hep3B-ST6Gal I (Figure 6A(*a*)) and control Hep3B (Figure 6A(*a'*)) cells, and the ST6Gal I localization was similar to that of the trans-Golgi marker adaptin γ (Figure 6A(*b*) and A(*b'*)). Following H_2O_2 treatment, both ST6Gal I and adaptin γ showed more disperse localizations, and more ST6Gal I was colocalized with the early endosome marker EEA1 (Figure 6A(*g*)). Since the level of endogenous BACE1 was below the level of detection in hepatic cell lines, we used Hep3B cells stably expressing BACE1-myc to examine the subcellular localization of BACE1. Since BACE1 was previously shown to be localized to the Golgi and endosomes (12), dispersed ST6Gal I following H_2O_2 treatment could possibly increase the ratio of the colocalized forms of ST6Gal I and BACE1. Indeed, following H_2O_2 treatment of Hep3B-BACE1 cells, more ST6Gal I was colocalized with BACE1 (Figure 6A(*o*)), which could result in enhanced ST6Gal I cleavage by BACE1. In these Hep3B cells, we failed to observe a striking increase in intracellular soluble

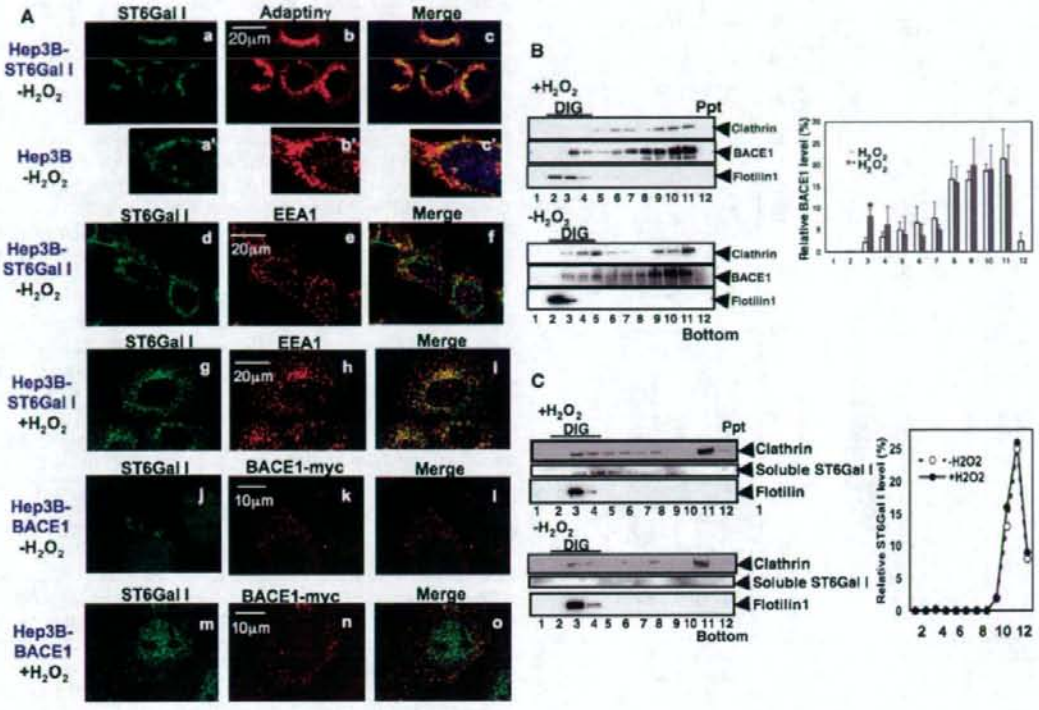

Fig. 6. Effects of H_2O_2 on the subcellular localizations of ST6Gal I and BACE1. (**A**) Hep3B cells (*a'–c'*) and Hep3B-ST6Gal I cells (*a–i*) for ST6Gal I detection and Hep3B-BACE1 cells for BACE1 detection (*g–o*) were left untreated (*a–f*, *a'–c'*, *j–l*) or treated with 40 μM H_2O_2 for 1 h (*g–i*, *m–o*). Hep3B and Hep3B-ST6Gal I cells were incubated with anti-ST6Gal I (M2) and anti-adaptin γ or anti-EEA1 monoclonal antibodies. Hep3B-BACE1 cells were incubated with anti-ST6Gal I (M2) and anti-myc monoclonal antibodies. In the merged images, DNA is stained with DAPI (blue). (**B**) HEK-BACE1 cells were treated with H_2O_2 (0 or 0.4 mM) for 1 h. After collection, the cells were solubilized and DRM fractions were isolated. Each fraction was subjected to SDS–PAGE and immunostaining with anti-BACE1, anti-clathrin heavy chain, and anti-flotillin 2 antibodies. Representative immunoblots are shown (left panel). Floating fractions containing DRMs are indicated by "DIG." The data represent the mean percentages of total BACE1 ± SEM ($n = 3$; right panel). $^*P < 0.01$. (**C**) From Hep3B-ST6Gal I cells grown at 33°C and treated with H_2O_2, DRM fractions were isolated as described in B. Representative immunoblots are shown in left panel. Right panel represent the mean percentages of total ST6Gal I quantified with the α2,6-sialyltransferase (M2) ELISA kit.

ST6Gal I, which appears to be consistent with our finding that increased ST6Gal I secretion following H_2O_2 treatment was only observed in primary hepatocytes. Owing to the technical limitation that no high-quality anti-BACE1 antibodies are available (Zhao et al. 2007), we failed to observe the change in the BACE1 localization by microscopic analysis. Nevertheless, our biochemical analyses suggested that BACE1 localization was also affected by H_2O_2 treatment. Since the production of Aβ from APP by BACE1 appears to be dependent on the lipid raft localization of APP and BACE1 (Simons et al. 1998; Ehehalt et al. 2003), we hypothesized that more BACE1 would be found in DRMs following H_2O_2 treatment. Therefore, we extracted H_2O_2-treated and untreated HEK-BACE1 cells with 1% Triton X-100 and performed floating analyses in stepwise sucrose gradients to separate the DRMs. Clathrin and flotillin 1 were detected as non-DRM and DRM marker proteins, respectively. In steady-state HEK cells, most of the BACE1 was found in the high-density non-raft fraction (Figure 6B). After H_2O_2 treatment, a significant amount of BACE1 was detected in the DRMs. Next, we extracted H_2O_2-treated and untreated Hep3B-ST6Gal I cells to separate DRMs and analyzed if cleaved ST6Gal I E41 form was found in the H_2O_2-treated cells. Although we detected all of the intact ST6Gal I molecules in the nonraft fraction (Figure 6C, right panel), we exclusively detected cleaved ST6Gal I E41 form in the DRMs of the H_2O_2-treated cells only grown at 33°C to decrease the secretion rate (Figure 6C, left panel). Taken together, the results suggest that oxidative stress caused increased colocalization of BACE and ST6Gal I in the DRMs, which would lead to simultaneous ST6Gal I cleavage to alter all of the intact ST6Gal I to its cleaved form.

Plasma ST6Gal I is increased in hepatitis patients

Next, we applied the α2,6-sialyltransferase (M2) sandwich ELISA system to samples from 88 hepatitis C patients. The level of serum ST6Gal I in patients with CAH was significantly increased compared to that in patients with CPH (Figure 7A, left panel). Furthermore, the level of ST6Gal I was highly correlated with the activity of hepatic inflammation (Figure 7B), but not with liver fibrosis (supplementary Figure S2). The ALT levels

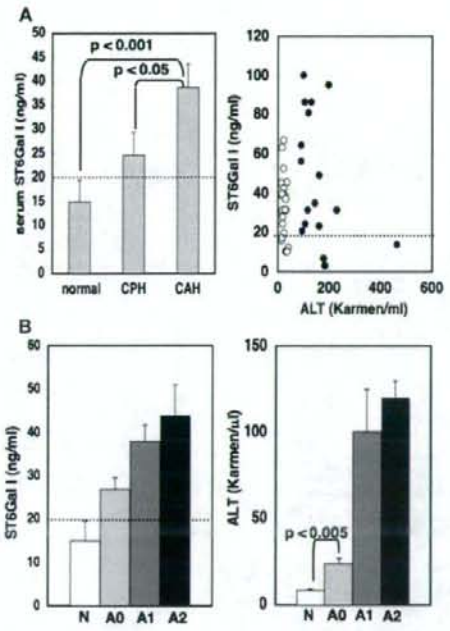

Fig. 7. Serum ST6Gal I levels in hepatitis patients. (**A**) The data for the serum ST6Gal I levels in healthy blood donors ($n = 21$), CPH patients ($n = 30$), and CAH patients ($n = 37$) are shown as the means ± SEM (left panel). The correlation between the levels of serum ST6Gal I and ALT is shown as a two-dimensional scatterplot (right panel). The horizontal dotted lines represent the cutoff value for hepatitis. (**B**) Data for the hepatitis marker ALT (right panel) and serum ST6Gal I (left panel) levels in healthy blood donors (N: $n = 18$) and hepatitis C patients with different necroinflammatory activities (grade A0: $n = 6$; grade A1: $n = 10$; grade A2: $n = 13$) are shown as the means ± SEM. The horizontal dotted line represents the cutoff value for hepatitis.

in A0 patients were significantly increased compared with those in healthy blood donors (N). Even though the level of ST6Gal I did not show such a significant increase in A0 patients, some of the A0 patients with lower ALT levels had elevated levels of ST6Gal I. These observations are consistent with our finding that the underlying molecular mechanism of enhanced ST6Gal I secretion is different from hepatic apoptosis/necrosis, by which plasma ALT is increased. When we set 20 ng/mL as the cutoff value (mean + SE) for ST6Gal I, none of the healthy blood donors were positive, while ~89% of A0 patients (8/9) and 100% of A1 patients (19/19) were positive.

Discussion

In the present study, we have shown that plasma ST6Gal I is increased in both zone 1 and zone 3 hepatocyte-injured rats. In each case, distinct molecular mechanisms were involved in the increases in soluble ST6Gal I in the plasma. In zone 1 hepatocyte-injured rats, acute phase reactions were elicited, and hepatic ST6Gal I expression was concomitantly increased. Using interleukin (IL)-6-deficient mice, a previous study clearly showed that ST6Gal I induction in the liver during acute phase reactions is predominantly mediated by an IL-6-dependent pathway (Dalziel et al. 1999). Induction of this inflammatory cytokine presumably mediates the elevation of both hepatic ST6Gal I expression and plasma ST6Gal I. In contrast, acute phase reactions were not elicited in zone 3 hepatocyte-injured rats, and oxidative stress appeared to be the trigger for ST6Gal I secretion instead, based on the following findings. We verified that H_2O_2 treatment did indeed stimulate the secretion of ST6Gal I E41 form by rat hepatocytes (Figure 5A). Oxidative stress did not induce the expression of either ST6Gal I or BACE1 (Figure 5B), but did change their intracellular localizations (Figure 6). There is growing evidence that the production of Aβ from APP by BACE1 (β-secretase) is partly regulated by the presence of both molecules in the same subcellular compartment, and Aβ processing appears to be dependent on the lipid raft localization of the APP substrate and the processing of β- and γ-secretase enzymes (Simons et al. 1998; Ehehalt et al. 2003). Notably, part of BACE1 was shifted to the DRMs by oxidative stress.

In the zone 1 hepatocyte-injured rats, plasma ST6Gal I was more sensitively increased than typical hepatitis markers, such as AST and ALT. In the zone 3 hepatocyte-injured rats, plasma ST6Gal I increased more rapidly than these hepatitis markers. The serum ST6Gal I levels decreased in the order of CAH patients to CPH patients to healthy blood donors. Some CAH patients had significantly elevated levels of ST6Gal I. The levels of both serum ST6Gal I and ALT were increased according to the necroinflammatory grade. It should be noted that some A0 grade patients with relatively low ALT levels exhibited significantly elevated serum ST6Gal I levels. These results highlight the possibility that monitoring plasma ST6Gal I in particular types of hepatitis B in which the levels of AST and ALT are not increased might be clinically useful (Bacon 2002). A previous study demonstrated that the localization of ST6Gal I is altered in hepatocellular carcinoma (Cao et al. 2002). This different ST6Gal I localization may possibly affect the ST6Gal I intracellular cleavage and plasma level of ST6Gal I. Therefore, we plan to apply our method to monitoring plasma ST6Gal I not only in acute hepatitis but also in chronic hepatitis, liver cirrhosis, and hepatocellular carcinoma in the future. Another interesting issue to clarify is how IL6-dependent ST6Gal I expression is controlled in hepatocarcinogenesis based on a recent report showing that ablation of IL-6 reduces the liver cancer risk in male mice (Naugler et al. 2007).

Materials and methods

Materials

Male Sprague-Dawley and Wistar rats maintained in specific pathogen-free conditions were purchased from Japan SLC Inc. (Shizuoka, Japan). The sources of the materials used in this study were as follows: tissue culture media and reagents, including DMEM, RPMI 1640 medium, and William's E medium (Invitrogen, CA, USA); protein molecular weight standards (Bio-Rad, CA, USA); and all other chemicals (Sigma, MO, USA or Wako Chemicals, Osaka, Japan). Protein concentrations were determined with BCA protein assay reagents (Pierce, IL, USA). The commercially available primary antibodies used in this study were anti-haptoglobin (rabbit polyclonal; Sigma), anti-α2-macroglobulin (goat polyclonal; ICN Co., OH, USA),

anti-4-hydroxy-2-nonenal (anti-4-HNE; mouse monoclonal; Japan Institute for the Control of Aging (JaICA, Shizuoka, Japan)), anti-heme oxygenase (mouse monoclonal; Abcam Ltd, Cambridge, UK), anti-BACE1 (rabbit polyclonal; Abcam Ltd), anti-myc (mouse monoclonal; Roche, Mannheim, Germany), anti-adaptin γ, anti-flotillin-2, anti-clathrin, and anti-early endosome antigen 1(EEA-1) (mouse monoclonal; BD Biosciences, CA, USA), and anti-glyceraldehyde-3-phosphate dehydrogenase (GAPDH) (mouse monoclonal; Chemicon, CA, USA). In addition, two different anti-ST6Gal I antibodies were used: E41 antibody specifically recognizing the cleaved form of rat ST6Gal I starting at Glu41 (Kitazume et al. 2001) and M2 antibody recognizing intact ST6Gal I. Both of these antibodies were produced by IBL-Japan Co. A series of sandwich ELISA systems, namely an α2,6-sialyltransferase (E41 form) sandwich ELISA kit, an α2,6-sialyltransferase (M2) sandwich ELISA kit, and a BACE1 ELISA kit, were also produced by IBL-Japan Co.

Serum samples and clinical diagnosis

The clinical study was approved by the Ethical Committee of Osaka University Graduate School of Medicine. Clinical diagnosis was made according to the serum alanine aminotransferase (ALT) levels (chronic persistent hepatitis (CPH): ALT<30 IU/L; chronic active hepatitis (CAH): ALT>100 IU/L). In patients who underwent a liver biopsy, histological evaluations were performed by two independent pathologists. The activity of inflammation was classified as A0–A3, and the level of fibrosis was classified as F0–F4.

Allyl alcohol (AA) and bromobenzene (BB) treatments

All experiments were performed in compliance with the Institutional Guidelines for Animal Experiments of RIKEN using rats weighing approximately 270 g after an overnight fast. AA (62 μmol/100 g body weight) dissolved in 250 μL of 0.9% NaCl or BB (380 μmol/100 g body weight) dissolved in 250 μL of corn oil was administered intraperitoneally. After each experiment, the rats were sacrificed by cardiac puncture under diethylether anesthesia. Following the removal of the liver, part of the tissue was fixed in 4% paraformaldehyde in 10 mM phosphate buffer (pH 7.4) and embedded in paraffin. Sections of the fixed tissue were stained with hematoxylin and eosin and subjected to histological examination.

Analysis of liver enzymes

The plasma levels of ALT and aspartate aminotransferase (AST) were measured using a Transaminase CII Test Kit (Wako Pure Chemical Industries) according to the manufacturer's protocol. The plasma levels of γ-glutamyl transpeptidase (γ-GTP) were measured using a γ-GTP C-test Kit (Wako Pure Chemical Industries).

Real-time quantitative PCR

Total RNA was isolated from rat livers using the Trizol reagent (Invitrogen). Subsequently, 5–10 μg of the RNA was reverse-transcribed with random hexamers using a SuperScript III RT Kit (Invitrogen) according to the manufacturer's protocol. The obtained cDNAs were amplified with 900 nM forward primer, 900 nM reverse primer, 250 nM fluorogenic probe, and 2.5 μL of Universal PCR Master Mix (Applied Biosystems, CA, USA) in a total volume of 20 μL using an ABI PRISM 7900HT sequence detection system (Applied Biosystems). The PCR conditions were 1 cycle of 50°C for 2 min and 1 cycle of 95°C for 10 min, followed by 40 cycles of 95°C for 15 s and 50°C for 1 min. All the primers and probes were purchased from Applied Biosystems. The sequences of the primers and probes for ST6Gal I were as follows: forward primer, 5′-CAGCAAGCAAGACCCTAAGGA-3′; reverse primer, 5′-CTGGAAGGAAGGCTGTGGTTT-3′; and probe, 5′-CCAATCCTCAGTTACCACAGGGTCACAGC-3′. For the BACE1 and GAPDH primers and probes, we used Assays-on-Demand Gene Expression Products, and the cDNAs were added to TaqMan Universal PCR Master Mix (Applied Biosystems), which contained all the reagents required for PCR. The probes for ST6Gal I and BACE1 were labeled with the fluorescent reporter dye FAM. The probes for GAPDH were labeled with VIC at their 5′-ends and the quencher dye TAMRA at their 3′-ends. The expression levels of the target genes were measured in duplicate and normalized to the corresponding GAPDH expression levels by the comparative C_T method following the instructions in User Bulletin 2 (Applied Biosystems).

Western blotting

We examined the plasma levels of α2-macroglobulin and haptoglobin by Western blot analysis following dilution in phosphate-buffered saline (PBS). We also analyzed the heme oxygenase levels in rat liver tissues following homogenization of rat liver samples in the T-PER buffer (Pierce) containing Complete Protease Inhibitor Cocktail (Roche). Liver homogenates and plasma samples were treated with the Laemmli sample buffer (Laemmli 1970), subjected to SDS–PAGE (5–20% acrylamide gradient gel) and transferred to nitrocellulose membranes. The membranes were incubated with anti-α2-macroglobulin (1:1000), anti-haptoglobin (1:1000), or anti-heme oxygenase (1:500) primary antibodies, followed by incubation with horseradish peroxidase (HRP)-conjugated anti-rabbit, anti-goat, or anti-mouse IgG secondary antibodies (Amersham Biosciences, NJ, USA). A chemiluminescent substrate (Pierce) was used for detection of antigen-antibody complexes (Kitazume et al. 2001). After detection of heme oxygenase, the membrane was washed with Restore Western Blot Stripping Buffer (Pierce) and incubated with the anti-GAPDH antibody. All signals were quantified using a Luminoimage Analyzer (LAS-1000 PLUS; Fuji Film, Tokyo, Japan).

Sucrose density gradient fractionation

Detergent-resistant membrane fractions (DRMs) were isolated from nearly confluent HEK cells stably expressing BACE1 or Hep3B-ST6Gal I cells. Briefly, cells grown in two 150 mm dishes were washed twice with PBS, scraped into 1 mL of lysis buffer (50 mM Tris-HCl, pH 7.4, 150 mM NaCl, 1% Triton X-100, Complete Protease Inhibitor Cocktail), homogenized by five passages though a 26-gauge needle and kept on ice for 1 h. Lysates were adjusted to a final sucrose concentration of 42.5% (final volume, 2 mL) and transferred to 11 mL ultracentrifuge tubes (13PA; Hitachi High-Technologies, Tokyo, Japan). A discontinuous sucrose gradient was formed by sequential layering of 30% sucrose (7 mL) and 5% sucrose (2 mL), and the tubes were ultracentrifuged at 34,000 rpm for 16 h in an RPS 40T rotor (Hitachi High-Technologies). Eleven 1 mL fractions were collected from the top, and the pellet was resuspended

in the buffer (50 mM Tris-HCl, pH 7.4, 150 mM NaCl, 0.1% Triton X-100, Complete Protease Inhibitor Cocktail) as the twelfth fraction. All fractions were concentrated with cold acetone and analyzed by SDS–PAGE and western blotting with anti-flotillin 1 (1:1000), anti-BACE1 (1:1000), anti-ST6Gal I E41 (1:100), and anti-clathrin heavy chain antibodies (1:1000) as described above.

Immunofluorescence

Liver sections were deparaffinized, washed twice with PBS, treated with the blocking solution (5% goat serum in PBS), and incubated with the anti-4-HNE monoclonal antibody diluted in Dako Antibody Diluent with Background Reducing Components (1:100 dilution) overnight at 4°C. After three rinses with PBS for 5 min each, the sections were incubated with Alexa Fluor 488-conjugated anti-mouse IgG (1:100 dilution; Molecular Probes) for 45 min. Rat hepatocytes maintained in the William's E medium containing 5% FBS, 1 nM insulin, and 1 nM dexamethasone were grown on collagen-type I-coated chamber slides (Iwaki). Rat hepatocytes were treated with 0 or 0.4 mM H_2O_2 for 1 h and fixed with ice-cold methanol for 15 min at −20°C. Hep3B cells stably expressing human BACE1-myc or ST6Gal I (Kitazume et al. 2001) hereafter referred to as Hep3B-BACE1-myc and Hep3B-ST6Gal I cells were maintained in RPMI/10% FBS containing 1.0 mg/mL G418 and grown on poly-L-lysine-coated chamber slides. Cells were treated with 0 or 40 μM H_2O_2 for 1 h, fixed with 4% paraformaldehyde, and then treated with 0.1% Triton X-100 for 1 min to detect BACE1-myc or fixed with 0.1% Tween 20 for 5 min to detect ST6Gal I. The fixed cells were incubated with anti-ST6Gal I E41 (1:40 dilution) or anti-ST6Gal I M2 (1:100 dilution) rabbit polyclonal antibodies plus anti-adaptin γ (1:50 dilution), anti-EEA1 (1:100 dilution), or anti-myc (1:100 dilution) mouse monoclonal antibodies. After washing, the cells were incubated with Alexa Fluor 488-conjugated anti-rabbit IgG (1:100 dilution; Molecular Probes) and Alexa Fluor 546-conjugated anti-mouse IgG (1:100 dilution; Molecular Probes, OR, USA). Following washing with PBS, the sections were mounted in the ProLong Gold antifade reagent containing DAPI (Invitrogen) and observed under an LSM510 Axiovert 100 M inverted microscope (Carl Zeiss) using a C-Apochromat (63×, 1.4 NA) oil immersion objective. Appropriate excitation and barrier filters were used to observe the fluorescence.

Quantification of ST6Gal I and BACE1

Plasma samples (7.5 μL) from mice, rats, and humans were analyzed for their soluble ST6Gal I levels using the α2,6-sialyltransferase (M2) sandwich ELISA kit, according to the manufacturer's protocol. For the rat samples, 7.5 μL plasma aliquots were also measured for their levels of soluble ST6Gal I starting at Glu41 using the α2,6-sialyltransferase (E41 form) sandwich ELISA kit. Hepatocytes (2.5×10^6 cells) were isolated from 10-week-old male Wistar rats by two-step collagenase perfusion (Seglen 1976), seeded on collagen-type I-coated plates (600 mm; Iwaki), and grown in William's E medium containing 5% FBS, 1 nM insulin, and 1 nM dexamethasone. After an overnight incubation, the cells were treated with H_2O_2 (0, 0.1, 0.2, 0.4, or 1 mM) for 0, 2, 4, 6, 8, or 20 h. At each time point, 100 μL of the medium was removed and centrifuged at $400 \times g$ for 5 min. Aliquots (50 μL) of the supernatants were measured for their soluble ST6Gal I levels using the α2,6-sialyltransferase (E41 form) sandwich ELISA kit. At 6 h after the H_2O_2 addition, the cells were lysed with the T-PER buffer containing Complete Protease Inhibitor Cocktail and analyzed with the α2,6-sialyltransferase (M2) ELISA kit or a BACE1 sandwich ELISA kit to detect intact ST6Gal I or BACE1, respectively.

Supplementary Data

Supplementary data for this article is available online at http://glycob.oxfordjournals.org/.

Funding

The New Energy and Industrial Technology Development Organization (NEDO) of Japan; the Ministry of Education, Science, Sports, and Culture of Japan (17046025 and 18570141 to S.K.); and the Ministry of Health, Labor and Welfare of Japan (2006-Nanchi-Ippan-017 to Y.H.).

Conflict of interest statement

None declared.

Abbreviations

AA, allyl alcohol; Aβ, amyloid β-peptide; ALT, alanine aminotransferase; APP, amyloid precursor protein; AST, aspartate aminotransferase; BACE, β-site APP-cleaving enzyme; BB, bromobenzene; CAH, chronic active hepatitis; CPH, chronic persistent hepatitis; DRM, detergent-resistant membrane fraction; EEA1, early endosome antigen 1; GAPDH, glyceraldehyde-3-phosphate dehydrogenase; γ-GTP, γ-glutamyl transpeptidase; 4-HNE, 4-hydroxy-2-nonenal; HRP, horseradish peroxidase; IL, interleukin; LEC, Long-Evans Cinnamon; PBS, phosphate-buffered saline; Sia, sialic acid; ST6Gal I, β-galactoside α2,6-sialyltransferase.

References

Aiso M, Takikawa H, Yamanaka M. 2000. Biliary excretion of bile acids and organic anions in zone 1- and zone 3-injured rats. *Liver.* 20:38–44.

Appenheimer MM, Huang RY, Chandrasekaran EV, Dalziel M, Hu YP, Soloway PD, Wuensch SA, Matta KL, Lau JT. 2003. Biologic contribution of P1 promoter-mediated expression of ST6Gal I sialyltransferase. *Glycobiology.* 13:591–600.

Bacon BR. 2002. Treatment of patients with hepatitis C and normal serum aminotransferase levels. *Hepatology.* 36:S179–S184.

Bennett BD, Denis P, Haniu M, Teplow DB, Kahn S, Louis JC, Citron M, Vassar R. 2000. A furin-like convertase mediates propeptide cleavage of BACE, the Alzheimer's {beta}-secretase. *J Biol Chem.* 275:37712–37717.

Bruix J, Boix L, Sala M, Llovet JM. 2004. Focus on hepatocellular carcinoma. *Cancer Cell.* 5:215–219.

Bussolati B, Ahmed A, Pemberton H, Landis RC, Di Carlo F, Haskard DO, Mason JC. 2004. Bifunctional role for VEGF-induced heme oxygenase-1 in vivo: Induction of angiogenesis and inhibition of leukocytic infiltration. *Blood.* 103:761–766.

Cao Y, Merling A, Crocker PR, Keller R, Schwartz-Albiez R. 2002. Differential expression of beta-galactoside alpha2,6 sialyltransferase and sialoglycans in normal and cirrhotic liver and hepatocellular carcinoma. *Lab Invest.* 82:1515–1524.